JOURNAL OF GUIDANCE, CONTROL, AND DYNAMICS
Vol. 17, No. 4, July–August 1994

Stationkeeping at Libration Points of Natural Elongated Bodies

Tomás Prieto-Llanos* and Miguel A. Gómez-Tierno†
Universidad Politécnica de Madrid, Madrid 28040, Spain

Collinear libration points are proposed as useful locations for the close survey of natural elongated bodies in rotation. The effect of the primary asphericity is introduced qualitatively by means of the mass dipole model, for which the equations of motion and the libration point stability analysis are derived as a generalization of the circular restricted three-body problem. A transformation is provided to obtain a linear mass distribution that is gravitationally equivalent to a body of revolution, and the results for the rotating dumbbell may be applied to a more general class of bodies. A modal control technique is described for stabilization of collinear libration points. This technique is then used to stabilize a simulated probe at *L*1 of the Mars-Phobos system.

Nomenclature

A_{mn} = moment mn of the potential
a = amplitude; semimajor axis
C = Jacobian constant
C_j = component of the jth mode
d = mass dipole length
e_j = direction of the jth mode in the position-velocity space
G = gravitational constant
H = Hamiltonian
k = parameter of angular rate of the rotating dipole, $MG/(\Omega^2 d^3)$
L_i = ith libration point
M = total mass of the primary
n = mean angular motion
O = center of mass of the primary
R = distance from the ξ-axis to a point of the body surface
r = distance from the ξ-axis to a point of V
S = primary body
U = gravitational potential
V = internal volume of the primary
v = velocity in the synodical frame
W = pseudopotential
w_{jkl} = coefficient jkl of the power series expansion of W
x, y, z = synodical co-ordinates of the secondary
κ = amplitude ratio of the synodical modes
λ = root of the characteristic equation
μ = linear mass density; mass ratio of the dipole
ξ, η, ζ = synodical co-ordinates of a point of the primary
Π = matrix of projection factors
π_{jk} = projection factor of the kth state component along the jth mode
ρ_j = distance from the secondary to the jth point mass of the primary
σ = mass density of the primary
τ = time constant of an exponential mode
φ = phase
Ω = angular rate of the primary
ω = pulsation frequency of the harmonic mode

Subscripts

1, 2 = first, second mass point of a dipole
e = exponential mode in the synodical plane
h = harmonic mode in the synodical plane
l, u = lower, upper bound
s = relative to the synodical plane
z = out of the synodical plane mode

Received May 22, 1992; revision received June 4, 1993; accepted for publication Aug. 2, 1993.

*Research Scientist, Departamento de Vehículos Aeroespaciales, E.T.S.I. Aeronáuticos, Cardenal Cisneros 3; currently Senior Staff Engineer, SENER, Madrid. Member AIAA.

†Associate Professor, Departamento de Vehículos Aeroespaciales, E.T.S.I. Aeronáuticos, Cardenal Cisneros 3; additionally Senior Staff, GMV, Madrid. Member AIAA.

I. Introduction

In the past decade, the space community has shown an increasing interest in exploring some celestial bodies (comet nuclei and the Mars satellite Phobos) that share the feature of being of elongated shape, an attribute common to other solar system objects such as Deimos, Amaltea (J5), J14 and, likely, some asteroids. Missions (such as Asteroid Gravity Optical and Radar Analysis (AGORA),[1] Comet Nucleus Sample Return (CNSR),[2] Comet Rendezvous and Asteroid Flyby (CRAF),[3] or the Soviet Phobos 88 mission), were analyzed or planned envisaging the close approach to, or even alighting on, these bodies.

The motion in the near vicinity of elongated bodies is influenced by both the central body mass distribution and its rotational behavior. A rotating system may have several libration points at which a mass point of negligible mass will remain at rest with respect to the rotating frame as centrifugal and gravitational accelerations cancel each other out and other inertial acceleration terms are null. One of these points has been already used, as the International Sun Earth Explorer ISEE-3 (see Ref. 4) librated about the sun-Earth $L1$ Lagrangian point. Moreover, control techniques[4–8] have been designed that result in efficient stationkeeping of libration point trajectories. In the case of a rotating elongated body, a probe initially placed near one of the libration points will remain in its neighborhood with little cost, even in the presence of perturbations. Therefore, libration points may turn out to be useful locations for the close survey of elongated bodies.

This paper studies the motion and control of a probe when in the proximity of the collinear libration points, i.e., those approximately aligned with the principal axis of lowest moment of inertia of the natural elongated body. A brief background is provided on models and dynamics of the primaries themselves. Equations of motion are obtained, mostly as a generalization of the circular restricted three-body problem (CRTBP).[9] Next, a station-keeping method is presented for maintenance at a

libration point. As an illustration, the stationkeeping at $L1$ of the Mars-Phobos system is simulated.

II. Primary

A. Rotational Dynamics

Regarding the rotational behavior, natural elongated bodies separate into bodies in pure rotation and nutating bodies. Asteroids and planetary satellites belong to the first class. They are old objects in the solar system and have reached the state of lowest energy for a given angular momentum, i.e., pure rotation about the principal axis of highest moment of inertia;[10] any primeval nutation faded away because nutation induces time-varying internal stresses that dissipate mechanical energy through hysteresis cycles.

Comet nuclei,[11] recent bodies in the solar system, form the second class. Mass loss around perihelion passage produces torques and modifies both the center of mass and the moment of inertia tensor, so nutation and precession appear.

B. Gravitational Field

The primary being considered in this paper is an elongated body. Its mass distribution differs greatly from the spherical one, the most common reference model in celestial mechanics. The usual gravitational potential expansion into spherical harmonics fails or needs a large number of terms in close proximity to the elongated body, and a different gravitational model is then required. In the model used by the authors, a body of revolution substitutes for the overall shape of revolution of the primary, while a set of mass points accounts for mean shape departures or mass concentrations (MASCONs).

III. Dynamics

A. Equations of Motion

Let us consider a point (the secondary) of negligible mass subject to the gravitational attraction of a primary body S that rotates with constant angular rate Ω about an axis Oz passing through its center of mass O. A sketch of this system is shown in Fig. 1. In the synodical frame $Oxyz$, rotating with the primary, the equations of motion of the point mass may be written as[5,9]

$$\begin{aligned} \ddot{x} - 2\Omega\dot{y} &= \frac{\partial W}{\partial x} \\ \ddot{y} + 2\Omega\dot{x} &= \frac{\partial W}{\partial y} \\ \ddot{z} &= \frac{\partial W}{\partial z} \end{aligned} \tag{1}$$

where the pseudopotential depends only upon position

$$W \triangleq \Omega(x^2 + y^2)/2 - U \tag{2}$$

and U is the gravitational potential

$$U = -G\iiint_V \sigma(\xi, \eta, \zeta)\,[(x-\xi)^2 + (y-\eta)^2 + (z-\zeta)^2]^{-1/2}\,d\xi d\eta d\zeta \tag{3}$$

The Hamiltonian is an integral of the motion, related to the Jacobian constant,

$$H = v^2/2 - W = \text{constant} = -C/2 \tag{4}$$

As v^2 is always positive, the secondary is restricted to stay within the surface of zero relative velocity of the motion, defined by $W = C/2$.

The equilibrium points in the synodical system satisfy

$$\nabla W = 0 \tag{5}$$

Although some of these equilibrium points are unstable, all of them are commonly called libration points.

The five Lagrangian points, equilibrium points of the circular restricted three-body problem (CRTBP) in which two mass point primaries revolve in circular Keplerian orbits around each other have been known since Euler and Lagrange's time. References 5 and 9 contain a detailed discussion of the different libration points and of the stability of motion in their vicinity.

In the case of a natural elongated body in rotation, the number, location, and stability of the libration points depend upon actual shape, mass distribution, and rotation period of the body. However, some qualitative information may be obtained from the study of a rotating mass dipole.

B. Rotating Dipole

Figure 2 presents the geometry of a problem in which the two point primaries of masses M_1 and M_2 are separated by a

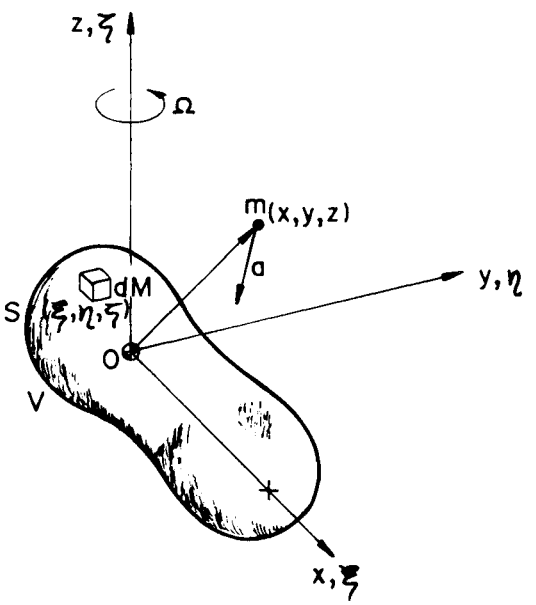

Fig. 1 Geometry of the problem: general case.

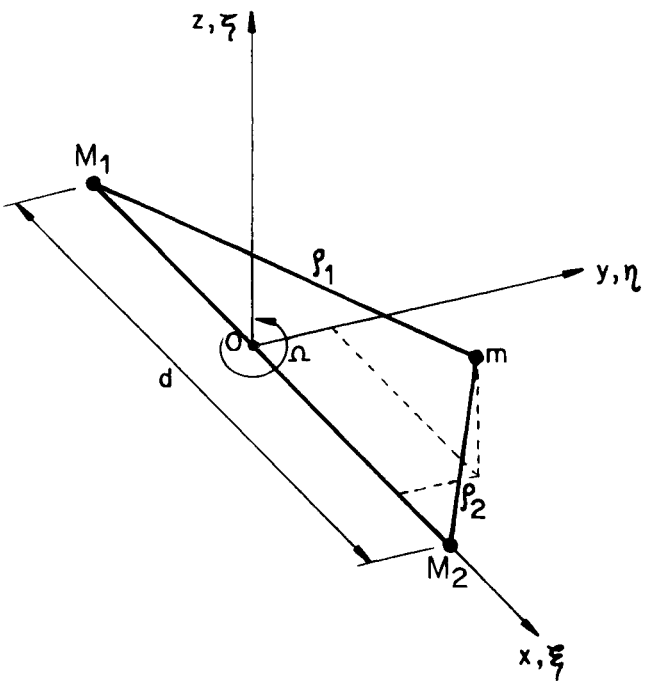

Fig. 2 Geometry of the problem: the rotating mass dipole.

constant distance d. This rotating dumbbell is a first approximation to an elongated body. After normalizing masses with the total mass of the dipole $M = M_1 + M_2$, lengths with the distance between primaries, and time with Ω^{-1}, the equations of motion become

$$\ddot{x} - 2\dot{y} = \frac{\partial W}{\partial x}$$
$$\ddot{y} + 2\dot{x} = \frac{\partial W}{\partial y} \tag{6}$$
$$\ddot{z} = \frac{\partial W}{\partial z}$$

where

$$W = (x^2 + y^2)/2 - U \tag{7}$$

$$U = -k[(1 - \mu)/\rho_1 + \mu/\rho_2] \tag{8}$$

$$\mu = M_2/M \in [0, 1], \qquad k = MG/(\Omega^2 d^3) \tag{9}$$

The parameter k is the ratio of gravitational acceleration to centrifugal acceleration. For $k = 1$, the problem becomes the classical CRTBP, a limiting case. For $k < 1$, cohesive strength is necessary to avoid body disruption under forces of inertia unbalanced by body self-gravitation; thence, the case $k < 1$ does not seem to be very realistic. Conversely, $k > 1$ should be the most frequent case, in which some compressive strength prevents the body from collapsing to adopt the shape of an oblate spheroid.

There are up to five libration points, all of them in the synodical plane. Three of them ($L1$, $L2$, and $L3$) are collinear with the primaries

$$Li = (x_{Li}, 0, 0), \qquad i \in \{1, 2, 3\} \tag{10}$$

lie within the range

$$x_{L1} \in]-\mu, 1-\mu[; \qquad x_{L2} \in]1-\mu, +\infty[; \qquad x_{L3} \in]-\infty, -\mu[\tag{11}$$

and satisfy Euler's quintic equation

$$\begin{aligned} &x_{Li}^5 + x_{Li}^4(4\mu - 2) + x_{Li}^3(6\mu^2 - 6\mu + 1) \\ &\quad + x_{Li}^2[4\mu^3 - 6\mu^2 + \mu(2 + k\{s_1 - s_2\}) - ks_1] \\ &\quad + x_{Li}[\mu^4 - 2\mu^3 + \mu^2(1 + 2k\{s_1 - s_2\}) - 4ks_1\mu + 2ks_1] \\ &\quad + k[\mu^3(s_1 - s_2) - 3\mu^2 s_1 + 3\mu s_1 - s_1] = 0 \end{aligned} \tag{12}$$

$$s_1 = \text{sign}\,(x + \mu), \qquad s_2 = \text{sign}\,(x - 1 + \mu) \tag{13}$$

Only $L2$ and $L3$ are suitable points to place a probe, since $L1$ would lie within the primary which the mass dipole approximates. However, $L1$ may be out of the primary in the case of a composed body (see example in Sec. V). The two remaining libration points (the triangular libration points $L4$ and $L5$) are equidistant from both primaries, and are placed at

$$L4, 5 = [1/2 - \mu, \pm (k^{2/3} - 1/4)^{1/2}, 0)] \tag{14}$$

C. Stability of the Libration Points

In the vicinity of a libration point, the linearized equations of motion are

$$\begin{aligned} \Delta\ddot{x} - 2\Delta\dot{y} &= 2w_{200}\Delta x + w_{110}\Delta y + w_{101}\Delta z \\ \Delta\ddot{y} + 2\Delta\dot{x} &= w_{110}\Delta x + 2w_{020}\Delta y + w_{011}\Delta z \\ \Delta\ddot{z} &= w_{101}\Delta x + w_{011}\Delta y + 2w_{002}\Delta z \end{aligned} \tag{15}$$

where the w_{jkl} are coefficients of the local power series expansion of W

$$W = W_o + \sum w_{jkl}\,(\Delta x)^j\,(\Delta y)^k\,(\Delta z)^l \tag{16}$$

1. *Collinear Libration Points*

In this case, the three nonnull coefficients in Eq. (15) are

$$w_{200} = (1 + 2A_{30})/2, \quad w_{020} = (1 - A_{30})/2, \quad w_{002} = -A_{30}/2 \tag{17}$$

where the moment A_{30} is given by

$$A_{mn} = k\,[(1 - \mu)\rho_1^{-m}(x_{Li} + \mu)^n + \mu\rho_2^{-m}(x_{Li} - \mu + 1)^n] \tag{18}$$

The z motion is harmonic, with pulsation frequency $\omega_z = (A_{30})^{1/2}$, and is not coupled with the synodical plane motion, for which the characteristic equation is

$$\lambda_s^4 + \lambda_s^2(2 - A_{30}) + (1 + 2A_{30})(1 - A_{30}) = 0 \tag{19}$$

Two roots are pure imaginaries and define a harmonic mode,

$$\begin{aligned} \Delta x &= a_h \cos(\omega_s t + \varphi_o) \\ \Delta y &= \kappa_h a_h \sin(\omega_s t + \varphi_o) \end{aligned} \tag{20}$$

$$\omega_s = |i\lambda_s|, \qquad \kappa_h = 2\omega_s/(A_{30} - 1 - \omega_s^2) \tag{21}$$

The two remaining roots τ_s^{-1} are opposite reals, and define exponential modes

$$(\Delta x, \Delta y) = a_e\, e^{t/\tau_s}\,(1, \kappa_e) \tag{22}$$

$$\kappa_e = (1 - (2A_{30} + 1)\tau_s^2)/2\tau_s \tag{23}$$

Since there is an exponential divergent mode, the collinear libration points are unstable, and active control is necessary to stay in their vicinity. Reference 12 contains series for the roots.

2. *Triangular Libration Points*

Now, the nonnull coefficients w_{jkl} in Eq. (15) are

$$\begin{aligned} w_{200} &= 3E/2, \qquad w_{020} = 3(1 - E)/2 \\ w_{002} &= -1/2, \qquad w_{110} = \pm 3(1 - 2\mu)(E - E^2)^{1/2} \end{aligned} \tag{24}$$

$$E = k^{-2/3}/4 \tag{25}$$

The z motion is harmonic, with $\omega_z = 1$, synchronous with the dipole rotation.

The characteristic equation of the motion in the synodical plane is

$$\lambda_s^4 + \lambda_s^2 + 36\mu(1 - \mu)\, E(1 - E) = 0 \qquad (26)$$

The system will be unstable when

$$144\mu(1 - \mu)\, E(1 - E) > 1 \qquad (27)$$

whereas it will otherwise present neutral stability. Figure 3 shows the stability domain in the $\mu - k$ plane. Two separate sufficient conditions for stability are

$$k \notin [((1/2 + \sqrt{2}/3)^{-3/2})/8, ((1/2 - \sqrt{2}/3)^{-3/2})/8], \quad \text{or}$$
$$\mu \notin [1/2 - \sqrt{2}/3, 1/2 + \sqrt{2}3/] \qquad (28)$$

that define a box excluding the region of unstable motion.

D. Axisymmetrical Body

Although a mass dipole may qualitatively introduce the effects of strong primary asphericity, such a simple model can hardly substitute for a generic body. However, an axisymmetrical body is able to more accurately represent an elongated primary. Furthermore, a body of revolution may be replaced by a linear mass distribution.

Let us consider a generic axisymmetrical body (Fig. 4) generated by revolving its meridian line $R(\xi)$, defined in the interval $\xi \in [\xi_l, \xi_u]$, about the axis of symmetry $O\xi$. The body has mass symmetry also, its density distribution depending upon the ξ-station and the distance r to the axis of symmetry

$$\sigma = \sigma(\xi, r), \qquad r \triangleq (\eta^2 + \zeta^2)^{1/2} \in [0, R(\xi)] \qquad (29)$$

A mass system equivalent to this body is the one-dimensional mass distribution, or mass rod, whose linear mass density $\mu(\xi)$ along 0ξ satisfies the integral equation derived hereafter. To be gravitationally equivalent to the body of revolution, a mass

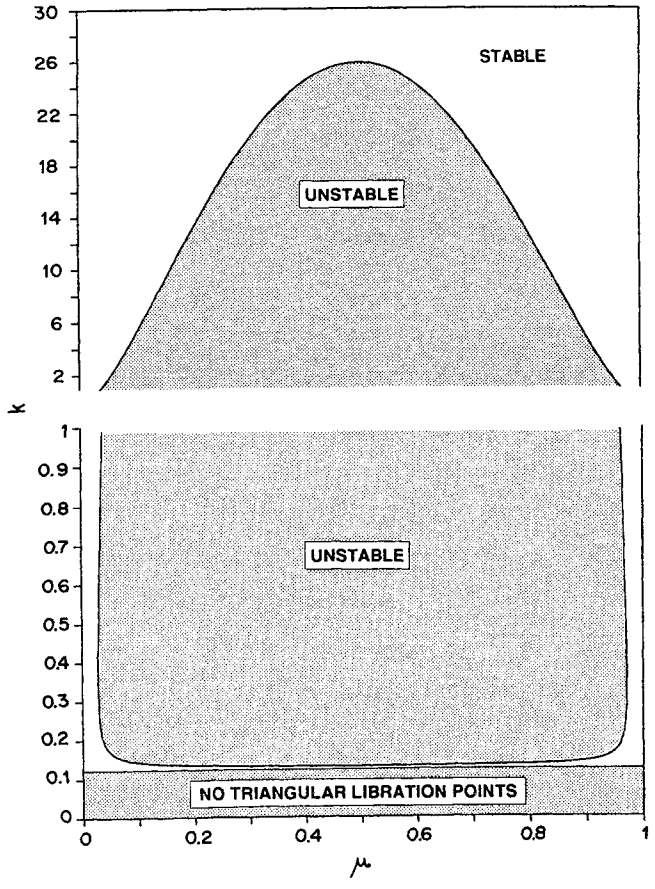

Fig. 3 Rotating mass dipole: *L*4, 5 stability domain.

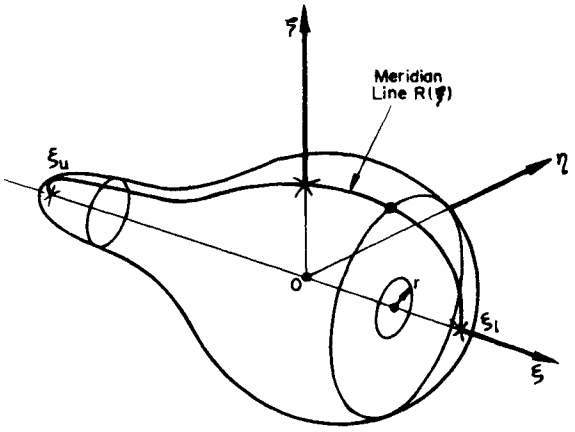

Fig. 4 Axisymmetrical body.

rod must produce the same gravitational potential as the body everywhere outside the body surface. This condition applies to axis $O\xi$ in particular, where the body gravitational potential is

$$f(x) = U(x, 0, 0) = -2\pi \int_{\xi l}^{\xi u}\int_{o}^{R} r\sigma(\xi, r)\,[(x - \xi)^2 + r^2]^{-1/2}\, dr d\xi \qquad (30)$$

and an integral equation to be satisfied by the linear mass distribution $\mu(x)$ is

$$f(x) = -\int_{\xi l}^{\xi u} [\mu(\xi/|x - \xi|]\, d\xi, \qquad x \in \boldsymbol{R} - [\xi_l, \xi_u] \qquad (31)$$

which forces the mass rod to produce the same gravitational potential $f(x)$ as the body of revolution along the axis of symmetry. Once the linear mass distribution has been obtained by solving Eq. (31), the gravitational potential it produces can be calculated as

$$U(x, y, z) = -k \int_{\xi l}^{\xi u} \mu(\xi)\,[(x - \xi)^2 + y^2 + z^2]^{-1/2}\, d\xi \qquad (32)$$

Although the number and location of the libration points will generally differ from those of the dipole, most of the results obtained for the mass dipole may be generalized to the linear mass distribution. All the relations relative to the stability of the collinear libration points [Eqs. (15–23)] remain valid with only the exception of Eq. (18), which is replaced by

$$A_{mn} = k \int_{\xi l}^{\xi u} \mu(\xi)\,[(x_{Li} - \xi)^2 + y_{Li}^2 + z_{Li}^2]^{-m/2}\,(x - \xi)^n\, d\xi \qquad (33)$$

where (x_{Li}, y_{Li}, z_{Li}) is the position vector of the libration point.

IV. Control of Collinear Libration Points

As collinear libration points are unstable, control is mandatory to stabilize a system subject to error sources, such as injection errors, state determination errors, maneuver mechanization errors, and model errors (on the gravitational model, nutation and precession of the primary, solar radiation pressure, ejection of gas and particles from the primary, etc.). This control shall be designed to also satisfy operational criteria such as avoidance of collision with the primary, low cost for stationkeeping, robustness, and autonomy (some of the natural frequencies may be so high that the time lag imposed by a remote control might destabilize the system).

Several control techniques have been devised for stationkeeping of a libration-point probe and for the orbit maintenance of halo orbits (quasiperiodical, three-dimensional orbits around a collinear libration point), with particular attention to the sun-

Earth and Earth-moon systems. Reference 5, a pioneering paper, proposed simple linear feedback control for stationkeeping as well as for homing after injection, and also discussed other controls (only-radial-axis control, on-off control, and stabilization by adjusting the length of a cable connecting two satellites).

In relation to the maintenance of halo orbits,[4,6-8] a shooting method that computes the maneuver to stay in the vicinity of a reference orbit until the next maneuver was applied to International Sun Earth Explorer ISEE-3 (See Ref. 4). Reference 6 proposes the use of optimal linear quadratic control to obtain the control gains; a reference orbit with much smaller residual acceleration than in Ref. 4 leads to a reduction in maneuver size. Reference 7 describes a modal control method that consists of three steps: the generation of a very accurate analytic reference orbit, the analysis of the dynamic behavior in the orbit neighborhood and, finally, the cancellation of the component along the unstable direction. Reference 8 extends a discrete-time optimal maneuver strategy method, originally developed for interplanetary multiple target missions, to stay in the vicinity of a numerically generated reference near-halo orbit. All these references declare results with similar maintenance cost of stationkeeping for halo orbits about $L1$ of the sun-Earth/Moon barycenter.

The controller used in this paper is a discrete-time controller derived from the one in Ref. 7, although the harmonic modes are controlled here also, and some heuristics are added to cope with relatively large model and measurement errors. At a generic control time, the probe state vector can be expressed in the local basis $\{e_j\}$, with components given by

$$C_j = \text{row}_j(\Pi) \cdot (x - x_{Li}, y - y_{Li}, z - z_{Li}, \dot{x}, \dot{y}, \dot{z})^T \quad (34)$$

The matrix of projection factors is built from the modes of the linear system and does provide an explicit expression (conversely to the system of Ref. 7)

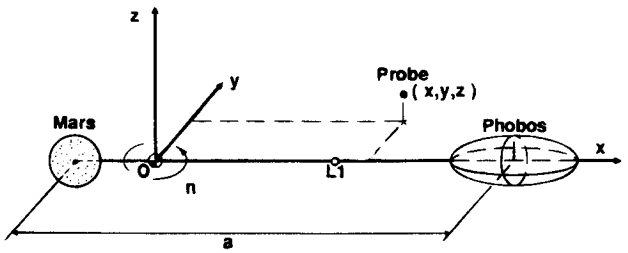

Fig. 5 Geometry of the problem: Mars-Phobos system.

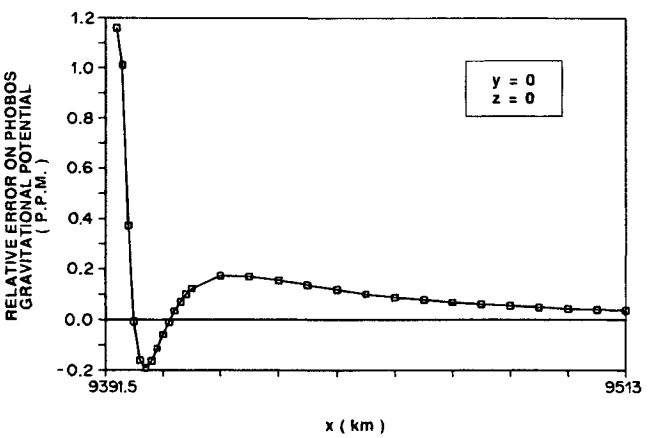

Fig. 6 Transformation from ellipsoid of revolution to set of ten mass points: relative error on Phobos' gravitational potential along the axis of symmetry.

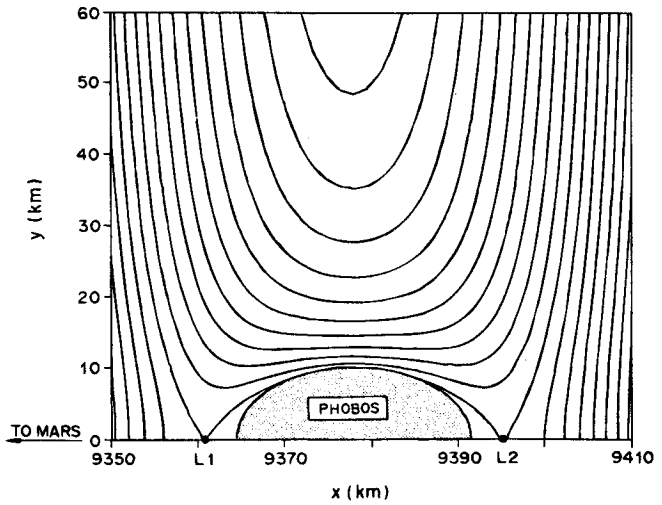

Fig. 7 Curves of zero relative velocity in the synodical plane of the Mars-Phobos system (level curves separated by 1 m^2/s^2).

Table 1 Effect of Phobos' shape on the parameters of dynamics

Parameter	Nominal	CRTBP
Phobos shape	Ellipsoid of revolution	Sphere
A_{30}, $1/s^2$	0.2415×10^{-6}	0.2082×10^{-6}
κ_e	−0.4901	−0.5390
τ_s, s	1592.	1747.
κ_h	−3.427	−3.212
ω_s, rad/s	0.5069×10^{-3}	0.4726×10^{-3}
ω_z, rad/s	0.4914×10^{-3}	0.4563×10^{-3}
χ_{L1}, km	9360.849	9361.879

Table 2 Mission and probe parameters

Parameter	Value
Duration	1 day
Interval between maneuvers	1200 s
Orbit determination error[a]	
random noise	10 m, 1 mm/s
bias	10 m, 1 mm/s
Injection error[a]	300 m, 30 cm/s
Maneuver mechanization error[a]	1 mm/s
Uncertainty of Phobos[b] gravitational model	$\pm 6.54 \times 10^{-5}$ km^3/s^2

[a] $1-\sigma$ along x, y, and z axes. [b] 10% of the nominal value.

Table 3 Effect of error sources on the delta-V budget

	Total ΔV, m/s			
Error Source	Mean	Std. dev.	Min.	Max.
Single error source				
- Orbit determination				
· Random noise (10 m, 1 mm/s)	1.13	0.12	0.76	1.42
· Bias (10 m, 1 mm/s)	0.41	0.31	0.03	1.51
- Injection error (300 m, 30 cm/s)	1.56	0.91	0.22	4.55
- Phobos gravitational model (+ 10% GM_{Phobos})				
Without $L1$ estimator	26.80	0.00	26.80	26.80
With $L1$ estimator	0.71	0.00	0.71	0.71
All the error sources	2.75	1.00	1.16	6.79

$$\Pi = [\pi_{jk}] = (e_1, \ldots, e_6)^{-1}$$

$$= \begin{bmatrix} 1 & 1 & 1 & 0 & 0 & 0 \\ \kappa_e & -\kappa_e & 0 & \kappa_h & 0 & 0 \\ 0 & 0 & 0 & 0 & 1 & 0 \\ 1/\tau_s & -1/\tau_s & 0 & -\omega_s\kappa_h & 0 & 0 \\ \kappa_e/\tau_s & \kappa_e/\tau_s & \omega_s\kappa_h & 0 & 0 & 0 \\ 0 & 0 & 0 & 0 & 0 & \omega_z \end{bmatrix}^{-1} \quad (35)$$

where the first row (π_{1k} corresponds to the unstable component.

An impulsive maneuver that cancels the jth component satisfies

$$(\pi_{jk}) \cdot (0, 0, 0, \Delta\dot{x}, \Delta\dot{y}, \Delta\dot{z})^T = -C_j \quad (36)$$

Since the maneuver affects only velocity, the six components C_j can not be zeroed at the same time, and the following control logic is used to choose which components are to be cancelled:

1. As in Ref. 7, the unstable component is cancelled without delay, as the control cost would otherwise increase, but the convergent exponential mode decays naturally and needs no control.
2. The component of the harmonic mode in the synodical plane is cancelled when the probe crosses the branch of the convergent mode.
3. The component of the harmonic mode along the z-axis is cancelled when the probe crosses the synodical plane.

Once the components to be zeroed are chosen, the optimal maneuver is the one that minimizes the Euclidean norm of the maneuver delta-V while zeroing these components, i.e., honoring the constraints of Eq. (36).

To deal with state determination and model errors, additional rules were introduced in the final version of our controller:

1. The true position of the libration point (that may in general differ from the a priori estimate) is estimated and then used when computing the C_j.
2. The amplitudes of the harmonic modes are not completely cancelled but reduced to a small value to excite (dither) the libration point estimator.
3. The maneuvers are applied only when the size exceeds a threshold (as in Ref. 6) chosen in accordance with the expected measurement errors.

V. Application: $L1$ of Mars-Phobos

We present an application to the station-keeping control of a probe at $L1$ of the Mars-Phobos system. This system does accept the treatment (modeling and controller design) described in previous sections, shows features from both the isolated elongated body and the CRTBP (Phobos is an elongated body permanently aligned with the other primary, Mars, of almost perfect spherical shape), and may turn out to be of practical interest in the future.

A. Mars-Phobos System

In this paper, a triaxial triellipsoid (of 27.0 × 21.6 × 18.8 km and a gravitational constant of 6.5385 × 10^{-4} km^3/s^2 ±

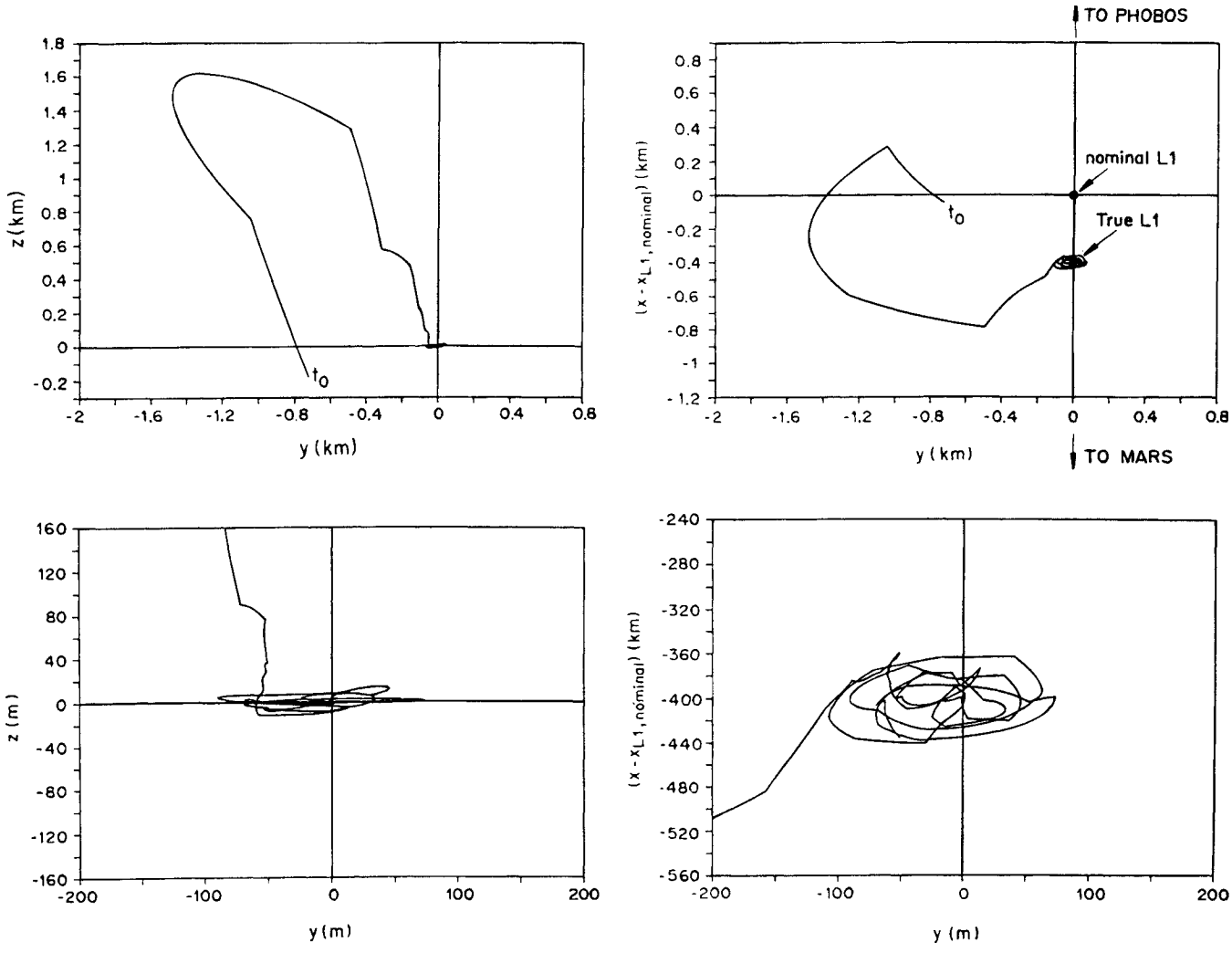

Fig. 8 Case of one-day stationkeeping at $L1$ of Mars-Phobos with + 10% error on Phobos mass: trajectory.

10%) substitutes for Phobos, whereas Mars is taken as a mass point 9378 km apart from Phobos and with a 42,828.3 km^3/s^2 gravitational constant. This model has already been used in a number of papers (e.g., Ref. 13). Given the small difference between two of the ellipsoid axes, Phobos may be approximated by an ellipsoid of revolution (of 27.0 km × 20.15ϕ km) orbiting Mars in a gradient stabilized attitude (Fig. 5). Now, the whole Mars-Phobos system presents the features of a body of revolution (the axis of symmetry is the line connecting the barycenters of the two bodies) which rotates with angular rate n, Phobos' mean angular motion about Mars. The system may be further replaced by the gravitationally equivalent linear mass distribution which satisfies Eq. (31). For practical reasons, an approximate solution, consisting of a set of mass points along the x-axis, is preferred to the exact solution to Eq. (31). Thus, one mass point has taken the place of Mars, whereas ten mass points substitute for Phobos. The approximation has a negligible contribution to model error. Just 4 km above Phobos' surface, the relative error introduced in the calculation of Phobos' gravitational potential falls below 10^{-6} (much smaller than the ±10% uncertainty in the mass of Phobos itself), and vanishes at infinity. Figure 6 presents the evolution of this error along the x-axis, the axis of revolution of the two bodies.

Figure 7 shows the curves of zero relative velocity of the Mars-Phobos system in the vicinity of Phobos. There are two libration points ($L1$ and $L2$) close to Phobos (nominally at 3.65 km altitude only). Notice that the mass distribution does allow an $L1$ solution because, conversely to the interior libration point of the rotating dipole of Sec. III. B, $L1$ does not lie within a primary. Three other libration points ($L3$, $L4$, and $L5$, none of them shown in Fig. 7) are in the positions corresponding to the classical CRTBP (i.e., at 18756, 9378, and 9378 km from Phobos, respectively), and one fictitious libration point is at Phobos' center. Consequently, $L1$ and $L2$ are the only practical static observation points close to Phobos, and, given the almost exact symmetry of the two libration points, only the stationkeeping at $L1$ will be considered. Table 1 compares the parameters of the nominal dynamics (ellipsoidal Phobos) with those of the CRTBP (spherical Phobos). The effect of Phobos asphericity is noticeable. In particular, $L1$ is 1 km (27% of $L1$ altitude) closer to Phobos' center in the CRTBP than in our nominal dynamics.

B. Controller

The technique described in Sec. IV. was used to design the controller. The expected gravitational mismodeling is likely to cause the true position of $L1$ to differ from the nominal position corresponding to nominal dynamics, and will similarly affect the projection factors. To deal with the effect of this error source, an on-board estimator of the true $L1$ position was implemented (with accuracy limited mainly by position measurement biases), whereas the updating of the projection factors was not required and the nominal ones were used. This approach was enough to drastically reduce the impact of model errors on station-keeping cost, while retaining control autonomy, low complexity, and low computational load.

C. Simulation Description

Batches of software simulations were performed for the mission and probe which are defined in Table 2. Two kinds of error sources were taken into consideration with pseudorandom errors, in accordance with the statistics of Table 2, representing the first kind:

1. The initial conditions of every simulation were obtained by perturbing the ideal injection (probe at rest in the nominal position of $L1$) with randomly generated injection errors affecting position and velocity.

2. On-board estimates of position and velocity were simulated by adding measurement biases (randomly generated at the beginning of every simulation) and white noise (randomly generated at every measurement time) to the actual values of every component of the probe state.

3. Orbital maneuvers were perturbed by randomly generated maneuver mechanization errors.

4. Gravitational mismodeling, introduced by placing a perturbing mass point (mass selectable by the user) at Phobos' center.

After generating the initial conditions, the state of the probe was propagated in the Mars-Phobos system (including a perturbing mass point at Phobos' center) until the first control time was reached. At that time, probe state and libration point position were estimated, and Eq. (34) provided the components of the state in the local basis using the aforementioned estimates and the nominal projection factors. The control logic decided whether to apply an impulsive maneuver and which components in the local basis were to be cancelled. If a maneuver was to be executed, maneuver mechanization errors were added to the ideal delta-V. Then the probe state was propagated to the next control time, and the procedure repeated until the final time was reached.

D. Results

The simulations allowed us to assess the sensitivity to single-error sources and determine the statistics of stationkeeping cost

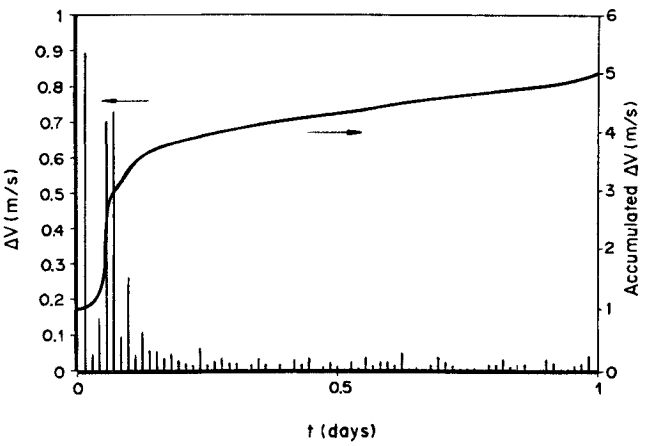

Fig. 9 Case of one-day stationkeeping at $L1$ of Mars-Phobos with + 10% error on Phobos mass: maneuver history.

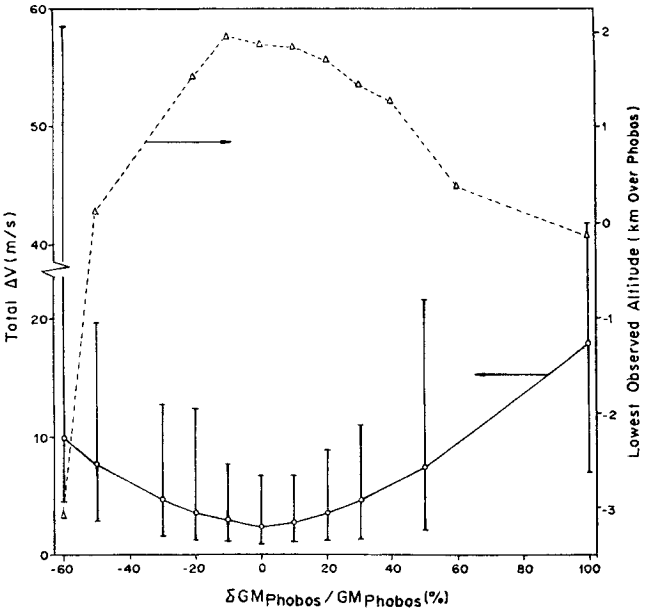

Fig. 10 Control robustness before Phobos mass model errors (one-day stationkeeping).

in the presence of all the error sources (see Table 3). The results are similar to the ones presented in Ref. 12, where linear quadratic control was applied to the stationkeeping at $L2$ of Mars-Phobos, as well as to the maintenance in a halo orbit about $L2$. A case of simulation is presented in detail in Figs. 8 (trajectory) and 9 (maneuver history). All the error sources were switched on, and an additional mass amounting to +10% of Phobos' mass was placed at Phobos' center. After the initial homing (costing some 4 m/s) towards the true $L1$, some 400 m farther from Phobos than the nominal $L1$, the probe stayed in the vicinity of the true $L1$ with a moderate cost of 1.5 m/s/day. Even in this case of large injection errors and relatively poor orbit determination accuracy, the delta-V expenditure seemed to be affordable.

Finally, Fig. 10 presents the effect of Phobos' mass uncertainty on station-keeping cost and on the lowest altitude reached (over the 1000 simulation cases run to generate each point/bar) in the presence of all the other error sources. Even employing nominal projection factors, the control was robust enough to tolerate model errors as large as 50% of the satellite mass without impacting on Phobos.

VI. Conclusions

The collinear libration points of natural elongated bodies in rotation have been proposed as a suitable location to place a probe. Generalizing from the classical restricted three-body problem, the stability of these points has been reviewed for the rotating mass dipole, considering especially the case in which both primaries are of similar mass and the angular rate does not correspond to Keplerian motion. A method is provided that transforms a body of revolution into a mass rod, which allows us to apply most of the results from a rotating mass dipole to rotating elongated bodies.

A modal control technique is described that stabilizes the collinear libration points. An application to the control of a probe at $L1$ of the Mars-Phobos system is presented in detail. The controller proves to be robust in the presence of large errors in the knowledge of the gravitational model, and well-suited for the close observation of natural elongated bodies, i.e., of small natural satellites (such as Phobos), asteroids, and comet nuclei.

Acknowledgment

The authors wish to thank J. Rodríguez-Canabal (European Space Agency/European Space Operations Centre, Darmstadt, Germany) for his valuable consultation and recommendations.

References

[1] Anon., "Asteroid Gravity Optical and Radar Analysis AGORA (Asteroid Gravity, Optical and Radar Analysis), Assesment Study," European Space Agency Rept. SCI(83)5, Sept. 1983.

[2] Anon., "The Comet Nucleus Sample Return Mission," European Space Agency Rept. SP-249, Dec. 1986.

[3] Draper, R. F., "The Mariner Mars II Program." AIAA Paper 88-0067, Jan. 1988.

[4] Farquhar, R. W., Muhonen, D., Newman, C., and Heuberger, H., "The First Libration Point Satellite. Mission Overview and Flight History," AAS/AIAA Astrodynamics Specialist Conference AAS/AIAA Paper 79–126, 1979.

[5] Farquhar, R. W., "The Control and Use of Libration—Point Satellites." NASA TR-R-346, Goddard Space Flight Center, Greenbelt, MD, Sept. 1970.

[6] Rodríguez-Canabal, J., "Operational Halo Orbit Maintenance Technique for SOHO," *Proceedings of The Second International Symposium on Spacecrafts Dynamics* (Darmstadt, Germany), European Space Agency SP-255, December, 1986, pp. 71–78.

[7] Simó, C., Gómez, G., Llibre, J., Martínez, R., and Rodríguez, J., "On The Optimal Stationkeeping Control of Halo Orbits," *Acta Astronautica*, Vol. 15, No. 6/7, 1987, pp. 391–397.

[8] Howell, K. C., and Pernicka, H. J., "A Stationkeeping Method for Libration Point Trajectories," AIAA Paper 90-2958, 1990.

[9] Szebehely, V., *Theory of Orbits. The Restricted Problem of Three Bodies*, Academic Press, 1967, pp. 7–40.

[10] McAdoo, D. C., and Burns, J. A., "Approximate Axial Alignment Times for Spinning Bodies," *Icarus*, Vol. 21, No. 1, 1974, pp. 86–93.

[11] Whipple, F. L., "The Rotation of Comet Nuclei," *Comets*, 1st ed., Univ. of Arizona Press, Tucson, AZ, 1982, pp. 227–250.

[12] Prieto-Llanos, T., "*Estudio de trayectorias útiles para la operación en las proximidades de un núcleo cometario*," Ph.D. Dissertation, Escuela Técnica Superior de Ingenieros Aeronáuticos, Univ. Politécnica de Madrid, Madrid, Spain, 1988.

[13] Dobrovolskis, A. R., and Burns, J. A., "Life Near The Roche Limit: Behavior of Eject from Satellites Close to Planets," *Icarus*, Vol. 42, No. 2, 1980, pp. 422–441.